Engineering Structures 179 (2019) 246–254

Contents lists available at ScienceDirect

Engineering Structures

journal homepage: www.elsevier.com/locate/engstruct

Cross laminated timber at in-plane beam loading – Comparison of model predictions and FE-analyses

Henrik Danielsson[a,*], Mario Jeleč[b], Erik Serrano[a], Vlatka Rajčić[c]

[a] Div of Structural Mechanics, Lund University, P.O. Box 118, SE-221 00 Lund, Sweden
[b] Department of Materials and Structures, University of Osijek, Croatia
[c] Department of Structures, University of Zagreb, Croatia

ARTICLE INFO

Keywords:
CLT
Beam
In-plane loading
Shear mode III
FE-analysis

ABSTRACT

The work presented concerns validation of a specific analytical model for Cross Laminated Timber (CLT) at in-plane beam loading conditions. The original model (model A) has previously been presented in the literature and is also suggested to be used as a basis for design equations for the next version of Eurocode 5. An improved version (model B) of that original model (model A), regarding basic assumptions relating to the internal force distribution, has recently been presented in the literature. Here, comparisons between the original model (model A), the improved model (model B) and FE-analyses regarding magnitude and distribution of internal forces are presented. The main focus is on forces and torsional moments acting in the crossing areas between longitudinal and transversal laminations and relevant for shear mode III failure, meaning the relative sliding and rotation between two flat-side bonded laminations. The results show that the improved analytical model (model B) outperforms the original model (model A) in terms of giving predictions very close to the predictions of the FE-model. A further extension of the improved model (model B) regarding distribution of forces and torsional moments in the beam width direction is also presented.

1. Introduction

The stress state in Cross Laminated Timber (CLT) at in-plane beam loading conditions is influenced by many geometry parameters and many failure modes need to be considered in design. Three failure modes need to be considered regarding strength verification with respect to shear: gross shear failure (mode I), net shear failure (mode II) and shear failure in the crossing areas between adjacent longitudinal and transversal laminations (mode III).

Several studies on CLT at shear loading are found in the literature. A comprehensive experimental investigation and design concepts of CLT diaphragms at shear loading has recently been presented by Brandner et al. [1]. The stress state differs, however, partly between in-plane loading of CLT diaphragms and CLT beams, for example regarding the stresses relevant for shear mode III failure. Several experimental investigations regarding CLT beams are found in the literature, see e.g. Jöbstl et al. [2], Bejtka [3], Andreolli et al. [4], Blaß & Flaig [5], Flaig [6] and Danielsson et al. [7,8].

An analytical model for CLT beams has been presented by Flaig [6,9–11] and by Flaig & Blaß [12], including proposals for stress based failure criteria for relevant failure modes. That model has also been used as a basis for design equations in the ongoing revision work of Eurocode 5 (EC5). Finite element (FE) analyses of CLT beams are also presented in [5,6,13], focusing on the beam bending strength as limited by parallel to grain normal stress in the longitudinal layers.

The analytical model of Flaig & Blaß does, however, suffer from some drawbacks relating to assumptions regarding distributions of internal forces and shear stresses acting in the crossing areas, as has been pointed out in [8,14,15]. Some alternative model assumptions and improvements of the original model, aimed at giving more accurate description of the internal force distribution, were recently presented by Danielsson & Serrano in [15]. Also the influence of the element lay-up in terms of the individual longitudinal layer thicknesses on the internal force distribution differ between the two considered models. The model by Danielsson & Serrano [15] has recently been used by Jelec et al. [16] to formulate proposals for design equations for CLT beams with respect to shear mode III failure.

The aim of this paper is to present a comparison of these two analytical models and 3D FE-analyses regarding magnitude and distribution of internal forces in CLT at in-plane beam loading conditions. The

* Corresponding author.
E-mail address: henrik.danielsson@construction.lth.se (H. Danielsson).
URL: http://www.byggmek.lth.se/english (H. Danielsson).

https://doi.org/10.1016/j.engstruct.2018.10.068
Received 26 June 2018; Received in revised form 20 September 2018; Accepted 24 October 2018
Available online 05 November 2018

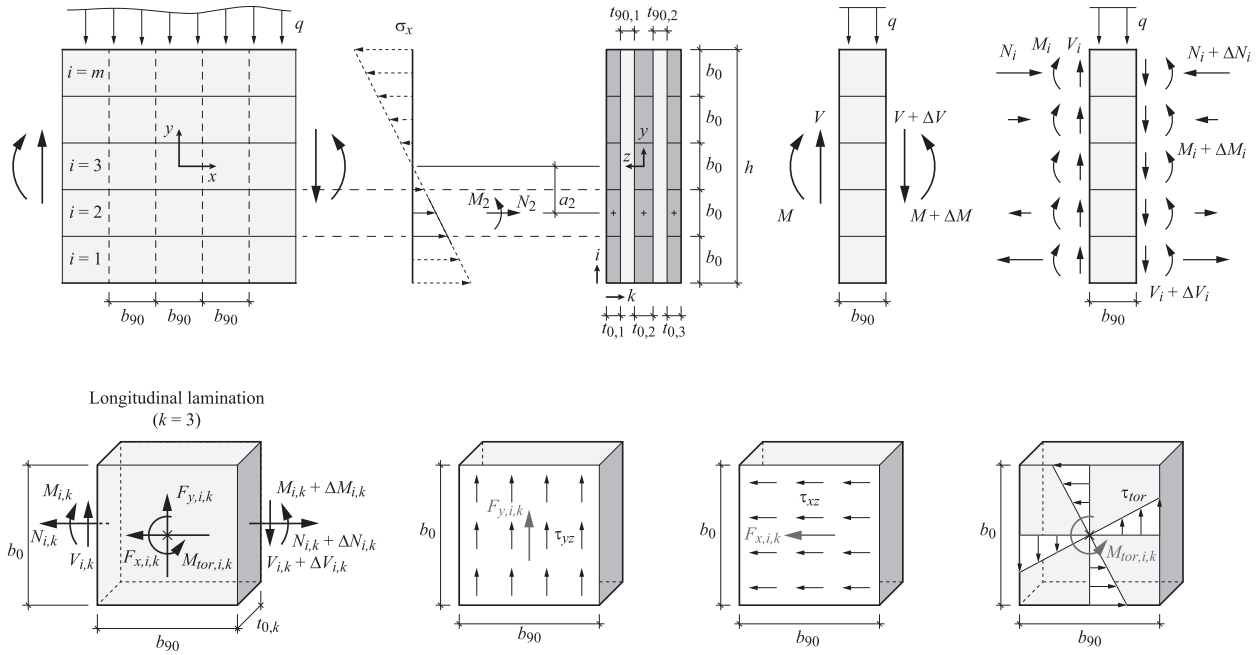

Fig. 1. Illustration of beam model and definition of load and geometry parameters.

main focus is placed on the forces and torsional moments acting in the crossing areas between longitudinal and transversal laminations which are relevant for shear mode III failure.

2. Analytical models

2.1. General

A CLT beam with geometry and load parameters according to Fig. 1 is considered. Equations presented below relate to prismatic CLT beams without edge-bonding and composed of transversal laminations of width b_{90} and longitudinal laminations of equal width b_0 and hence having an integer number of longitudinal laminations, $m = h/b_0$, in the beam height direction. Index i refers to the position of the longitudinal laminations in the beam height direction and index k refers to the position of the longitudinal and transversal layers in the beam width direction.

Cross section forces and bending moments are considered at three separate levels according to Fig. 1: (V, N, M) refer to the forces and the bending moment acting on the total cross section, (V_i, N_i, M_i) refer to the sum of forces and bending moments acting in all k longitudinal laminations for a certain i and ($V_{i,k}$, $N_{i,k}$, $M_{i,k}$) refer to the forces and the bending moment acting in an individual longitudinal lamination i, k.

A linear normal strain distribution is assumed in the beam height (y) direction. Due to no edge-bonding between adjacent laminations and due to the low stiffness perpendicular to grain compared to parallel to grain, normal stress parallel to the beam axis, σ_x, is assumed to be present in the longitudinal laminations only. The normal stress σ_x is further assumed to be uniformly distributed in the beam width (z) direction. Shear stresses τ_{xy} are present in both longitudinal and transversal laminations. Since elements without edge-bonding are considered, all narrow faces of the laminations are traction-free.

Shear stresses τ_{xz} and τ_{yz} act in the crossing areas between the longitudinal and transversal laminations. These shear stresses can be decomposed into stresses due to three basic in-plane loading situations: (a) shear stress parallel to the beam axis τ_{xz}, (b) shear stress perpendicular to the beam axis τ_{yz} and (c) torsional shear stress τ_{tor}. The corresponding resulting forces $F_{x,i,k}$ and $F_{y,i,k}$ and the torsional moment $M_{tor,i,k}$ are illustrated in Fig. 1 where also the assumed shear stress distribution according to the model by Flaig & Blaß are shown.

2.2. Original model – Model A

Flaig & Blaß suggest that the forces and torsional moments acting in the crossing areas, with sufficient accuracy, can be taken as uniformly distributed in the beam width direction irrespective of the element lay-up in terms of the individual longitudinal layer thicknesses $t_{0,k}$ for CLT made of softwoods and with lay-ups as used in practice. Their model is further based on assumptions of equal torsional moments for all crossing areas in the beam height direction, which corresponds to assuming equal lamination shear forces in the beam height direction, i.e. $V_i = V/m$.

The parallel to beam axis force $F_{x,i,k}$ and the corresponding shear stress component $\tau_{xz,i,k}$ can according to [12], with sufficient accuracy, be expressed as

$$F_{x,i,k} = \frac{12Vb_{90}}{m^3 b_0^2}\frac{1}{n_{CA}}a_i \tag{1}$$

$$\tau_{xz,i,k} = \frac{F_{x,i,k}}{b_0 b_{90}} = \frac{12V}{m^3 b_0^3}\frac{1}{n_{CA}}a_i \tag{2}$$

where

$$a_i = b_0\left(\frac{m+1}{2} - i\right) \tag{3}$$

and where n_{CA} is the total number of crossing areas in the beam width direction, i.e. n_{CA}= 2, 4 and 6 for CLT beams with 3, 5 and 7 layers, respectively.

The torsional moment $M_{tor,i,k}$ and the corresponding torsional shear stress component $\tau_{tor,i,k}$ can according to [12], with sufficient accuracy, be expressed as

$$M_{tor,i,k} = \frac{Vb_{90}}{n_{CA}}\left(\frac{1}{m} - \frac{1}{m^3}\right) \tag{4}$$

$$\tau_{tor,i,k} = \frac{M_{tor,i,k}}{I_{P,CA}}\frac{b_{max}}{2} = \frac{3V}{b_0^2}\frac{1}{n_{CA}}\left(\frac{1}{m} - \frac{1}{m^3}\right)\frac{2b_0 b_{max}}{b_0^2 + b_{90}^2} \tag{5}$$

where

$$I_{P,CA} = \frac{b_0 b_{90}}{12}(b_0^2 + b_{90}^2) \tag{6}$$

and where $b_{max} = \max\{b_0, b_{90}\}$.

2.3. Improved model – Model B

With respect to the original model of Flaig & Blaß, the model improvements presented by Danielsson & Serrano in [15] include: (a) consideration of the influence of the element lay-up in terms of the individual longitudinal layer thicknesses $t_{0,k}$ on the stress distribution in the beam width direction and (b) consideration of an uneven distribution in the beam height direction of the torsional moments $M_{tor,i,k}$, which is a consequence of an uneven distribution in the beam height direction of the lamination shear forces $V_{i,k}$.

At locations in the beam length direction corresponding to a section in-between adjacent transversal lamination, the shear force V must be carried by the longitudinal laminations only. The distribution of the total shear force V over the individual longitudinal laminations can be expressed as

$$V_{i,k} = \alpha_i \beta_k V \tag{7}$$

where α_i and β_k are dimensionless weighting factors describing the distribution of the shear force in the beam height (α_i) and the beam width (β_k) directions. Weighting factors α_i according to

$$\alpha_i = \frac{6i - 6i^2 + m(6i - 3) - 2}{m^3} \tag{8}$$

are proposed in [15], based on the parabolic shear stress distribution found from conventional engineering beam theory for a homogeneous beam of height $h = mb_0$ and width $t_{net,0} = \sum t_{0,k}$. A distribution in the beam width direction based on the individual longitudinal layer thicknesses $t_{0,k}$ according to

$$\beta_k = \frac{t_{0,k}}{t_{net,0}} \tag{9}$$

is further proposed in [15].

The parallel to beam axis force $F_{x,i,k}$ and the corresponding shear stress component $\tau_{xz,i,k}$ can according to [15] be expressed as

$$F_{x,i,k} = \frac{12Vb_{90}}{m^3 b_0^2} \frac{t_{0,k}}{t_{net,0}} \frac{1}{n_{CA,k}} a_i \tag{10}$$

$$\tau_{xz,i,k} = \frac{F_{x,i,k}}{b_0 b_{90}} = \frac{12V}{m^3 b_0^3} \frac{t_{0,k}}{t_{net,0}} \frac{1}{n_{CA,k}} a_i \tag{11}$$

where $n_{CA,k}$ is the number of crossing areas that the individual longitudinal lamination shares with adjacent transversal laminations, i.e. $n_{CA,k} = 1$ or 2.

The torsional moment $M_{tor,i,k}$ and the corresponding torsional shear stress component $\tau_{tor,i,k}$ can according to [15] be expressed as

$$M_{tor,i,k} = \frac{Vb_{90}}{n_{CA,k}} \left(\alpha_i \beta_k - \frac{t_{0,k}}{t_{net,0}} \frac{1}{m^3} \right) \tag{12}$$

$$\tau_{tor,i,k} = \frac{M_{tor,i,k}}{I_{P,CA}} \frac{b_{max}}{2} = \frac{3V}{b_0^2} \frac{1}{n_{CA,k}} \left(\alpha_i \beta_k - \frac{t_{0,k}}{t_{net,0}} \frac{1}{m^3} \right) \frac{2b_0 b_{max}}{b_0^2 + b_{90}^2} \tag{13}$$

3. Numerical model

Full 3D FE-analyses were carried out in order to study the internal force distribution in CLT at in-plane beam loading. Results of the numerical model are compared with the original analytical model of Flaig & Blaß [12] (model A) and the improved model of Danielsson & Serrano [15] (model B). CLT beams composed of 3 layers (3s) and 5 layers (5s) are considered in the study, with beam geometries as illustrated Fig. 2.

The laminations were modelled as linear elastic and orthotropic with stiffness parameters according to Table 1. The rectilinear material directions are denoted by L in the lamination length direction, T in the width direction and R in the thickness direction. Adjacent laminations within the same layer were modelled with a gap of width t_{gap} = 0.2 mm. The flat-wise bonding between the laminations was modelled using a combination of hard contact in compression and elastic response in tension perpendicular to the crossing areas and in the two shear directions. The linear elastic traction-separation model used a single stiffness value for all three directions, $K_{nn} = K_{tt} = K_{ss}$= 1000 N/mm^3, for tension and the two shear directions, respectively. The FE-analyses were performed using Abaqus 2017 [17] and 8-node linear brick elements (C3D8 in Abaqus) were used. Symmetry in the beam width (z) direction was considered and the FE-meshes consisted mostly of cubically, or close to cubically, shaped elements having a side length of about 5 mm.

The widths of the individual longitudinal and transversal laminations were consistently $b_0 = b_{90}$ for all geometries. Most analyses were performed on a reference beam geometry of CLT 5s and with lamination widths $b_0 = b_{90}$ = 150 mm, m = 4 longitudinal laminations in the beam height direction and 7 transversal laminations in the beam length direction. For the CLT 5s beam geometries, a longitudinal net cross section width $t_{net,0} = \sum t_{0,k}$ = 120 mm was consistently considered.

A parameter study concerning various beam geometry parameters was carried out to study the influence on the internal force distribution in the laminations and in the crossing areas. The longitudinal layer thicknesses were varied within the ranges $26 \leqslant t_{0,1} = t_{0,3} \leqslant 52$ mm and $16 \leqslant t_{0,2} \leqslant 68$ mm in such a way that the relative longitudinal layer thicknesses were varied within the range $0.31 \leqslant t_{0,2}/t_{0,1} = t_{0,2}/t_{0,3} \leqslant 2.62$. Transversal layer thicknesses $t_{90,1} = t_{90,2}$ = 10, 20 and 40 mm were considered giving ratios of longitudinal to transversal net cross section widths within the range $1.5 \leqslant t_{net,0}/t_{net,90} \leqslant 6.0$. Analyses were performed considering m = 3, 4, 5 and 6 longitudinal laminations in the beam height direction and with lamination widths then being $b_0 = b_{90}$ = 200, 150, 120 and 100 mm, respectively. A beam part of length $L \approx 2h$ and consisting of an odd number of transversal laminations in the beam length direction was considered for all analyses.

Loads were applied to the individual longitudinal laminations at the two respective ends of the CLT beam. The applied loads were in equilibrium and the model was only constrained to prevent rigid body motions. Shear forces V = 15,000 N and bending moments $M_L = M_R = M = VL/2$ were applied, giving zero bending moment (pure shear) at a section through the middle of the centre-most transversal lamination. The loads on the individual laminations were applied according to assumptions of the analytical model as presented in [15] and may hence be expressed as

$$N_{i,k} = \frac{12M}{m^3 b_0^2} \frac{t_{0,k}}{t_{net,0}} a_i \tag{14}$$

$$M_{i,k} = \frac{M}{m^3} \frac{t_{0,k}}{t_{net,0}} \tag{15}$$

$$V_{i,k} = \alpha_i \beta_k V \tag{16}$$

with α_i and β_k according to Eqs. (8) and (9).

Presented results relate to the lamination shear forces $V_{i,k}$, the torsional moments $M_{tor,i,k}$ and the parallel to beam axis forces $F_{x,i,k}$. The forces and moments are evaluated in laminations and in the crossing areas according to Fig. 2, at a beam section around the centre-most of the odd number of transversal laminations in the beam length direction. Forces and moments from the FE-analyses were determined by integration of the stresses over the relevant areas.

Results are in the following partly presented as the sum of the forces over the k layers of laminations/crossing areas in the beam width direction and over the i laminations/crossing areas in the beam height direction according to the following notation

$$V_i = \sum_k V_{i,k} = \begin{cases} V_{i,1} + V_{i,2} & \text{for 3s} \\ V_{i,1} + V_{i,2} + V_{i,3} & \text{for 5s} \end{cases} \tag{17}$$

$$V_k = \sum_{i=1}^{m} V_{i,k} = V_{1,k} + V_{2,k} + ... + V_{m,k} \tag{18}$$

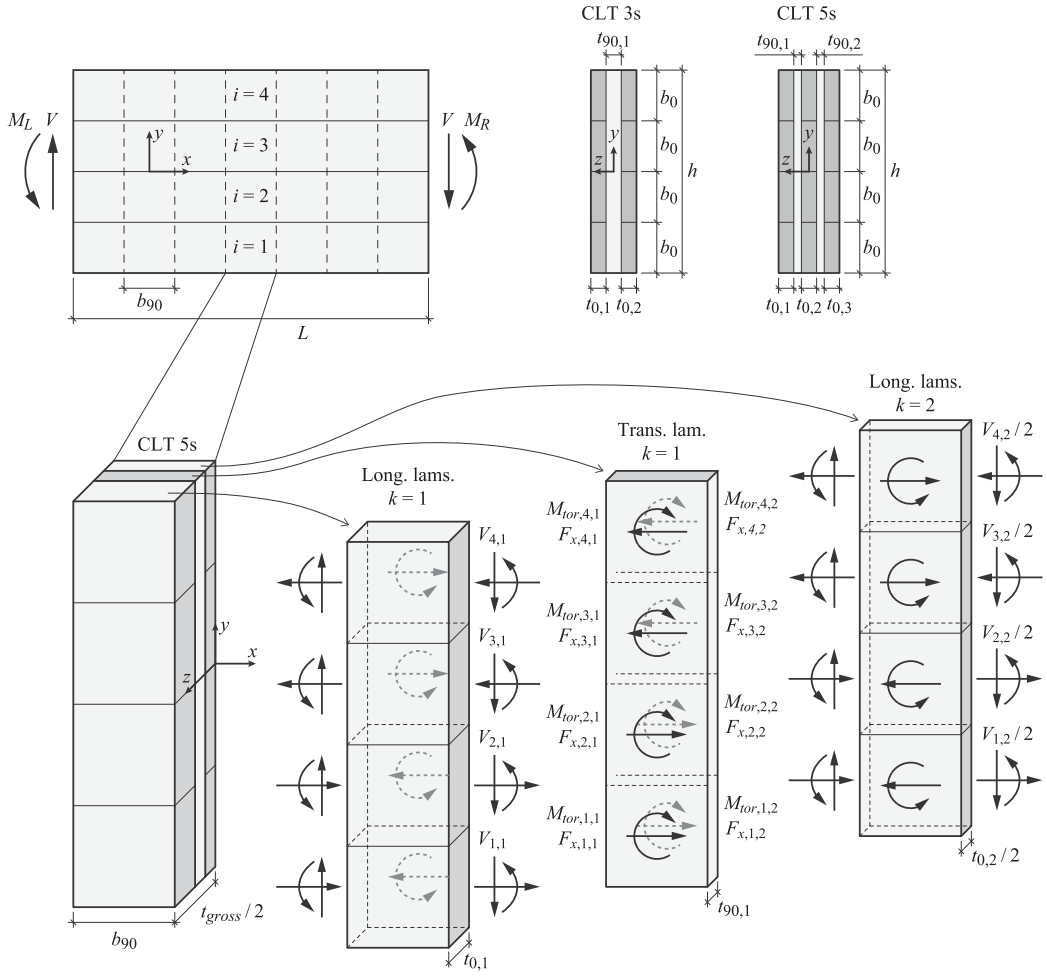

Fig. 2. Illustration of considered beam geometry for FE-analysis.

Table 1
Lamination stiffness parameters used for FE-analyses.

E_L [MPa]	E_T [MPa]	E_R [MPa]	G_{LT} [MPa]	G_{LR} [MPa]	G_{TR} [MPa]	ν_{LT} [–]	ν_{LR} [–]	ν_{TR} [–]
12,000	400	600	750	600	75	0.50	0.50	0.33

$$V_{tot} = \sum_{i=1}^{m} V_i \tag{19}$$

$$M_{tor,i} = \sum_{k} M_{tor,i,k} = \begin{cases} M_{tor,i,1} + M_{tor,i,2} & \text{for 3s} \\ M_{tor,i,1} + 2M_{tor,i,2} + M_{tor,i,3} & \text{for 5s} \end{cases} \tag{20}$$

$$M_{tor,k} = \sum_{i=1}^{m} M_{tor,i,k} = M_{tor,1,k} + M_{tor,2,k} + \ldots + M_{tor,m,k} \tag{21}$$

$$M_{tor,tot} = \sum_{i=1}^{m} M_{tor,i} \tag{22}$$

$$F_{x,i} = \sum_{k} F_{x,i,k} = \begin{cases} |F_{x,i,1}| + |F_{x,i,2}| & \text{for 3s} \\ |F_{x,i,1}| + 2|F_{x,i,2}| + |F_{x,i,3}| & \text{for 5s} \end{cases} \tag{23}$$

$$F_{x,k} = \sum_{i=1}^{m} F_{x,i,k} = |F_{x,1,k}| + |F_{x,2,k}| + \ldots + |F_{x,m,k}| \tag{24}$$

$$F_{x,tot} = \sum_{i=1}^{m} F_{x,i} \tag{25}$$

4. Results

A preliminary parameter study of the influence of the type of load application, the contact stiffness parameters and the mesh density was performed considering CLT 3s with results presented in Section 4.1. A more comprehensive parameter study of the influence of the element lay-up and the number of longitudinal laminations in the beam height direction was performed considering CLT 5s and results are presented in Sections 4.2–4.5. Forces and torsional moments according to the FE-analyses as described in Section 3 are compared with forces and torsional moments according to the analytical models A and B as presented in Sections 2.2 and 2.3, respectively.

4.1. Preliminary parameter study – CLT 3s

A beam geometry CLT 3s with $b_0 = b_{90} = 150$ mm, $m = 4$ and lay-up (40–20–40), i.e. $t_{0,1} = t_{0,2} = 40$ mm and $t_{90,1} = 20$ mm, is considered here. The reference case for this parameter study is based on load application, contact stiffness parameters and mesh density as stated in Section 3. Six alternative variations of load application, stiffness parameters and mesh densities are considered within this parameter study:

Load alternative a
Lamination forces and bending moments according to Eqs. (14)–(16), with $\alpha_i = 1/m$ and hence uniform distribution of the total shear force V over the i longitudinal laminations in the beam height direction.
Load alternative b

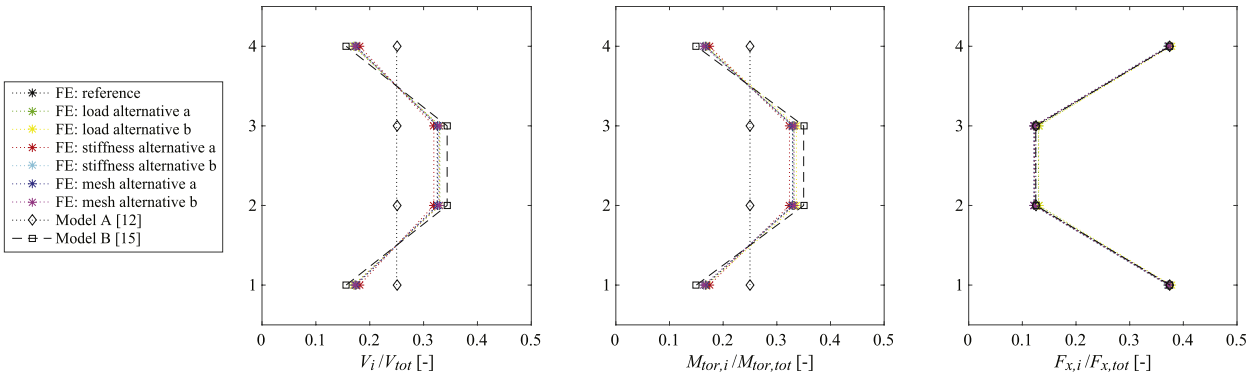

Fig. 3. Comparison for internal forces and moments according to FE-analyses and analytical models for CLT beam 3s with $m = 4$ longitudinal laminations in the beam height direction and element lay-up (40–20–40). Definition of forces and moments according to Fig. 2 and Eqs. (17)–(25).

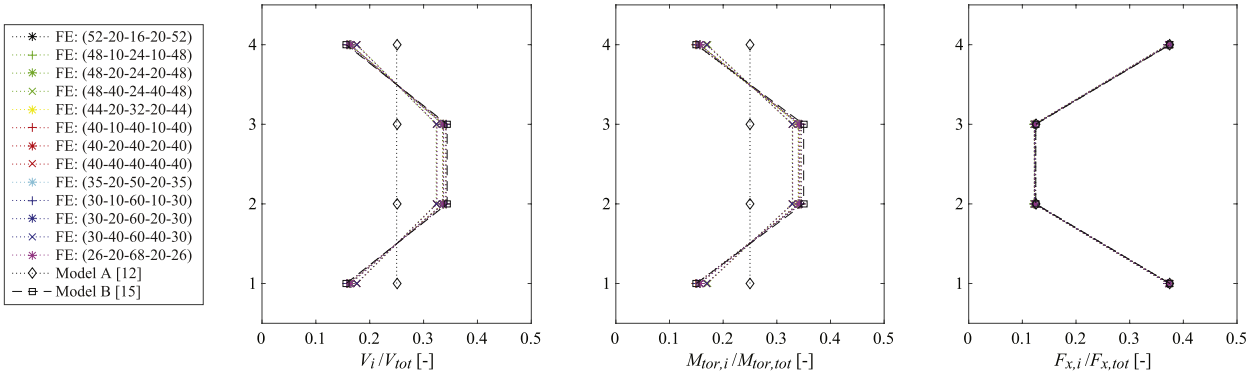

Fig. 4. Distribution in beam height direction of internal forces and moments according to FE-analyses and analytical models for CLT 5s with $m = 4$ longitudinal laminations in the beam height direction and lay-ups ($t_{0,1}$–$t_{90,1}$–$t_{0,2}$–$t_{90,2}$–$t_{0,3}$). Definition of forces and moments according to Fig. 2 and Eqs. (17)–(25).

Lamination shear forces $V_{i,k}$ according to Eq. (16), lamination bending moments $M_{i,k} = 0$ and lamination axial forces $N_{i,k}$ giving a total bending moment $M = \sum_{i=1}^{m} N_{i,1} a_i + \sum_{i=1}^{m} N_{i,2} a_i = VL/2$.

Stiffness alternative a

Contact stiffness parameters as $K_{nn} = K_{tt} = K_{ss} = 100\,\text{N/mm}^3$.

Stiffness alternative b

Contact stiffness parameters as $K_{nn} = K_{tt} = K_{ss} = 10{,}000\,\text{N/mm}^3$.

Mesh density alternative a

Overall element side length 4 mm.

Mesh density alternative b

Overall element side length 10 mm.

Results of these seven FE-analyses in terms of shear forces, torsional moments and parallel to beam axis forces are presented in Fig. 3. The forces and moments are equal for the two layers of longitudinal laminations and the two crossing areas in the beam width direction since the considered beam is composed of only two longitudinal layers and due to symmetry. Results are hence presented for V_i, $M_{tor,i}$ and $F_{x,i}$ only.

Only minor differences in terms of calculated forces/moments are found for the FE-analyses with different types of load application, different contact stiffness properties and for the different FE-mesh densities. The ratios between the forces/moments according to the six FE-analyses with alternative input parameters and the forces/moments of the reference FE-analysis are 0.97–1.04 for V_i, 0.98–1.04 for $M_{tor,i}$ and 0.99–1.07 for $F_{x,i}$. By comparison of results according to the reference case and load alternatives a and b, it can be seen that the distributions of the applied loads at the two beam ends seem to have only a very small influence on the internal force distribution at the sections where the forces are evaluated (i.e. around the center-most transversal laminations).

Forces and torsional moments according to analytical models A and B as presented in Sections 2.2 and 2.3, respectively, are also shown in Fig. 3. Uniform distribution of the torsional moments $M_{tor,i,k}$ and the shear forces $V_{i,k}$ over the beam height, as assumed in model A, is in clear disagreement with the FE-results. In contrast, distributions of $M_{tor,i,k}$ and $V_{i,k}$ based on model B with α_i according to Eq. (8) agree well with the results from the FE-analyses. Eqs. (1) and (10) for the parallel to beam axis force $F_{x,i,k}$ are identical for CLT 3s and are in good agreement with the results of the FE-analyses.

4.2. Distribution of forces in the beam height direction – CLT 5s

Distribution of forces and moments in the beam height direction for CLT 5s with $m = 4$ longitudinal laminations in the beam height direction and individual laminations widths $b_0 = b_{90} = 150$ mm are presented in Fig. 4 for different lay-ups. The presented forces and moments are V_i, $M_{tor,i}$ and $F_{x,i}$ according to the definitions in Eqs. (17)–(25).

The distributions of $V_{i,k}$ and $M_{tor,i,k}$ in the beam height direction are in good agreement with analytical model B. The ratios between the forces and moments according to the FE-analyses and according to this analytical model are 0.94–1.13 for V_i, 0.94–1.14 for $M_{tor,i}$ and 0.98–1.00 for $F_{x,i}$. Considering the maximum values, the corresponding ratios are 0.94–0.99 for $\max\{V_i\}$, 0.94–0.99 for $\max\{M_{tor,i}\}$ and 0.99–1.00 for $\max\{F_{x,i}\}$. The respective distributions in the beam height direction are not much influenced by the relative longitudinal layer thicknesses $t_{0,2}/t_{0,1} = t_{0,2}/t_{0,3}$ nor by the relative net cross section widths $t_{net,0}/t_{net,90}$, within the limits studied here.

Distribution of forces and moments in the beam height direction for CLT beams with $3 \leqslant m \leqslant 6$ longitudinal laminations in the beam height direction and with lay-up (40–20–40–20–40) are presented in Fig. 5. Also here good agreement is found between results of the FE-analyses and analytical model B. Thus it seems that Eqs. (7), (8), (10) and (12) are suitable to describe the distribution of forces and moments in the beam height direction.

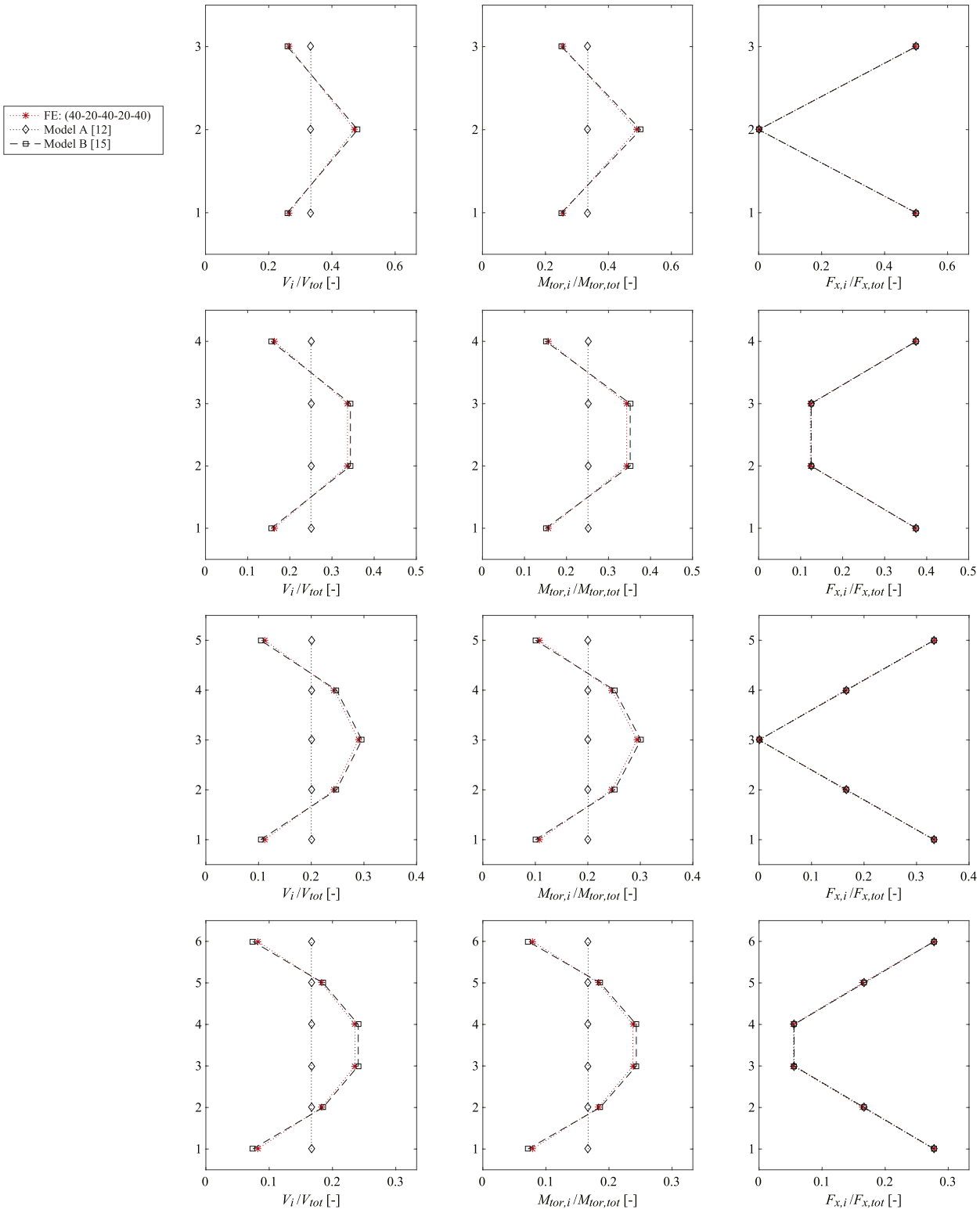

Fig. 5. Distribution in beam height direction of internal forces and moments according to FE-analyses and analytical models for CLT 5s with $3 \leqslant m \leqslant 6$ longitudinal laminations in the beam height direction and element lay-up (40–20–40–20–40). Definition of forces and moments according to Fig. 2 and Eqs. (17)–(25).

The assumptions of equal lamination shear forces and equal torsional moments for all crossing areas in the beam height direction, see analytical model A and Eq. (4), are clearly in disagreement with the results of the FE-analyses.

4.3. Distribution of forces in the beam width direction – CLT 5s

Distribution of forces and moments in the beam width direction for CLT 5s with $b_0 = b_{90} = 150$ mm and $m = 4$ longitudinal laminations in the beam height direction are presented in Fig. 6 for different lay-ups. The considered forces and moments are V_k, $M_{tor,k}$ and $F_{x,k}$ according to the definitions in Eqs. (17)–(25).

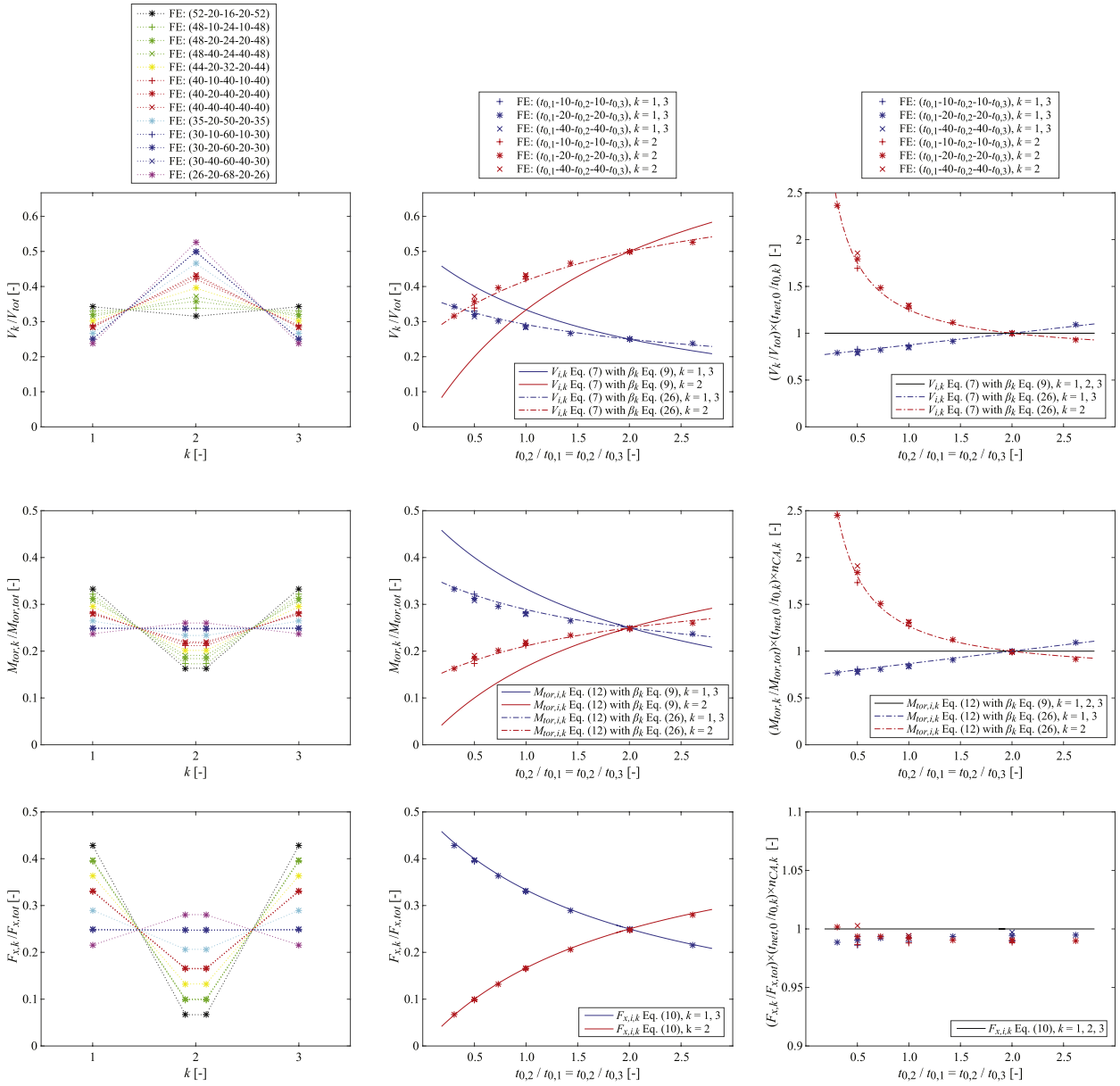

Fig. 6. Distribution in beam width direction of internal forces and moments according to FE-analyses and analytical models for CLT 5s with m = 4 longitudinal laminations in the beam height direction and lay-ups ($t_{0,1}$–$t_{90,1}$–$t_{0,2}$–$t_{90,2}$–$t_{0,3}$). Definition of forces and moments according to Fig. 2 and Eqs. (17)–(25).

As can be seen in Fig. 6, the distribution of the lamination shear forces found from the FE-analyses differ partly compared to the assumptions used in analytical model B with β_k according to Eq. (9). The ratios between the shear forces V_k according to the FE-analyses and according to this analytical model are 0.93–2.36 for V_2 and 0.79–1.09 for V_1 and V_3 for the wide range of CLT lay-ups used within the parameter study, with $0.31 \leqslant t_{0,2}/t_{0,1} = t_{0,2}/t_{0,3} \leqslant 2.62$. For $t_{0,2}/t_{0,1} = t_{0,2}/t_{0,3} = 2.0$, i.e. an interior longitudinal layer thickness twice the external longitudinal layer thicknesses, the lamination shear forces found from the FE-analyses agree very well with the assumed shear force distribution. For $t_{0,2}/t_{0,1} = t_{0,2}/t_{0,3} \leqslant 2.0$, however, the FE-analyses give distributions of the laminations shear forces where a comparatively larger part of the total shear force is carried by the centric layer (k = 2) and a comparatively smaller part is carried by the external layers (k= 1 and 3). As for the shear forces V_k, discrepancies between the results of the FE-analyses and analytical model B are also found for the torsional moments $M_{tor,i,k}$.

Regarding the parallel to beam axis forces $F_{x,i,k}$ and their distribution in the beam width direction, a very good agreement between the FE-analyses and analytical model B can be observed in Fig. 6. The ratios between the parallel to beam axis forces $F_{x,k}$ according to the FE-analyses and according to Eq. (10) are 0.99–1.00 for $F_{x,1}$, $F_{x,2}$ and $F_{x,3}$ for the wide range of CLT lay-ups used within the parameter study.

The distributions in the beam width direction of the considered forces and moments found from the FE-analyses are not much influenced by the element lay-up in terms of the relative net cross section widths $t_{net,0}/t_{net,90}$ within the limits studied.

The assumption of equal forces $F_{x,i,k}$ for all crossing areas in the beam width direction irrespective of the element lay-up, see analytical model A and Eq. (1), is clearly in disagreement with the results of the FE-analyses. Also the assumption of equal torsional moments $M_{tor,i,k}$ for all crossing areas in the beam width direction, see analytical model A and Eq. (4), is in disagreement with the results of the FE-analyses, however, not quite to the same extent as for $F_{x,i,k}$.

4.4. Alternative weighting factors β_k – CLT 5s

The distribution of the lamination shear forces $V_{i,k}$ is of importance

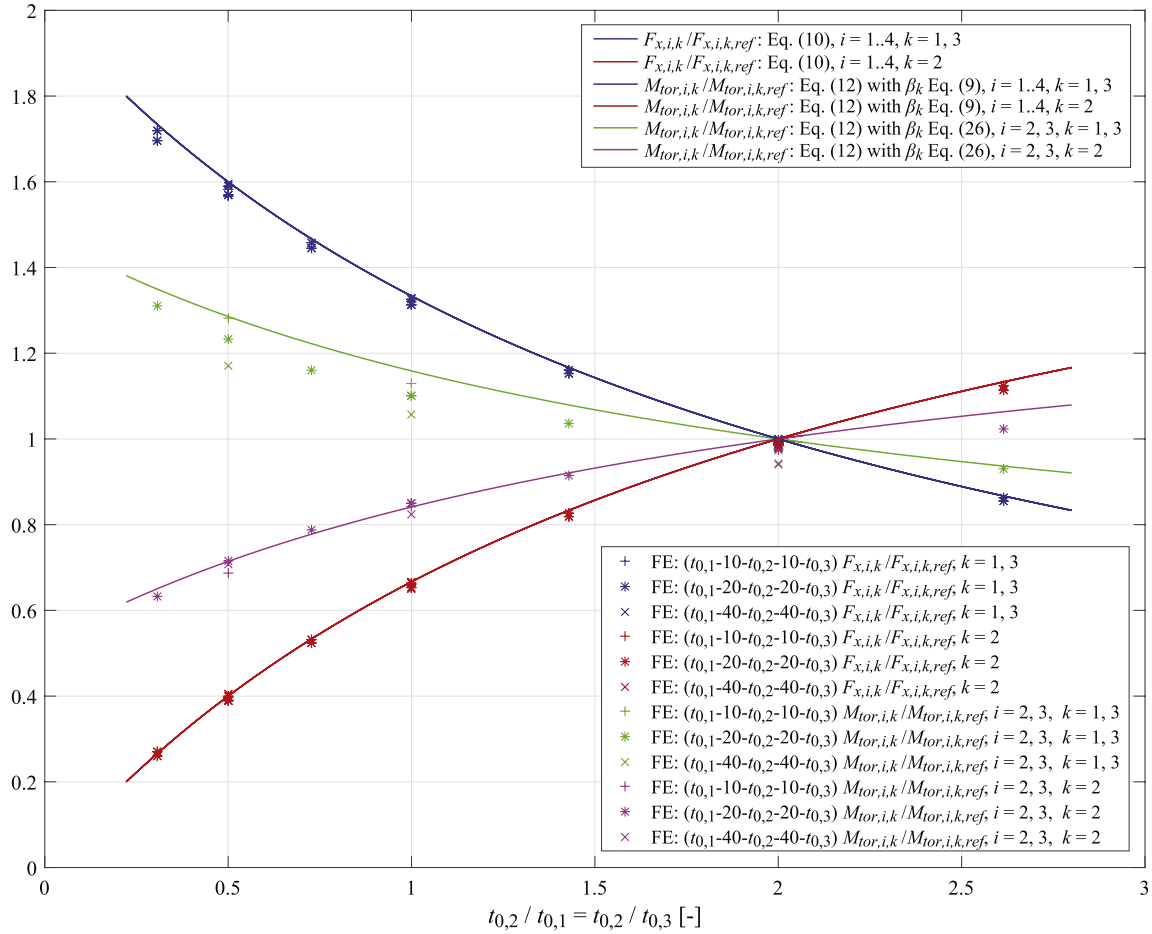

Fig. 7. Comparison for forces $F_{x,i,k}$ and torsional moments $M_{tor,i,k}$ for CLT 5s with $m = 4$ longitudinal laminations in the beam height direction, individual lamination widths $b_0 = b_{90} = 150$ mm and lay-ups ($t_{0,1}$–$t_{90,1}$–$t_{0,2}$–$t_{90,2}$–$t_{0,3}$). The forces and moments are normalized with respect to reference forces $F_{x,i,k,ref}$ according to Eq. (10) and torsional moments $M_{tor,i,k,ref}$ according to Eq. (12) considering a lay-up with $t_{0,2}/t_{0,1} = t_{0,2}/t_{0,3} = 2.0$.

in relation to the stress state in the crossing areas and thus for design with respect to shear mode III failure, since α_i and β_k determine the torsional moments $M_{tor,i,k}$ and the torsional shear stresses $\tau_{tor,i,k}$, see Eqs. (12) and (13). Based on manual curve-fitting of the lamination shear forces V_k found from the FE-analyses as presented in Fig. 6, alternative expressions for the weighting factors β_k were determined according to

$$\beta_k = \begin{cases} \frac{1}{8}\left(1 + 4\frac{t_{0,k}}{t_{net,0}}\right) & \text{for } k = 1, 3 \\ \frac{1}{4}\left(1 + 2\frac{t_{0,k}}{t_{net,0}}\right) & \text{for } k = 2 \end{cases} \tag{26}$$

with $\sum_{k=1}^{3} \beta_k = 1.0$. Distributions of V_k and $M_{tor,k}$ based on β_k according to Eq. (26) are shown in Fig. 6.

4.5. Overall comparison of forces in crossing areas – CLT 5s

Individual torsional moments $M_{tor,i,k}$ and parallel to beam axis forces $F_{x,i,k}$ are presented in Fig. 7 for the FE-analyses of CLT 5s with $m = 4$ longitudinal laminations in the beam height direction, individual lamination widths $b_0 = b_{90} = 150$ mm and different lay-ups ($t_{0,1}$–$t_{90,1}$–$t_{0,2}$–$t_{90,2}$–$t_{0,3}$). The forces and moments are normalized with respect to reference forces $F_{x,i,k,ref}$ according to Eq. (10) and torsional moments $M_{tor,i,k,ref}$ according to Eq. (12) considering a reference lay-up with $t_{0,2}/t_{0,1} = t_{0,2}/t_{0,3} = 2.0$.

Forces $F_{x,i,k}$ are given for all crossing areas while torsional moments $M_{tor,i,k}$ are given only for the most centrically placed crossing areas ($i = 2, 3$). Data points for $k = 1$ and $k = 3$ are identical due to symmetry in the beam width direction and data points for $i = 1, 4$ and $i = 2, 3$, respectively, are (almost) identical due to symmetry in the beam height direction.

For the parallel to beam axis forces $F_{x,i,k}$, an overall very good agreement between the results of the FE-analyses and analytical model B and Eq. (10) can be observed for all considered element lay-ups. The ratios between the parallel to beam axis forces $F_{x,i,k}$ found from the FE-analyses and as given by Eq. (10) are 0.97–1.01.

For the torsional moments $M_{tor,i,k}$, the overall agreement between the FE-results and analytical model B is worse. The influence of the element lay-up in terms of the relative longitudinal layer thicknesses $t_{0,2}/t_{0,1} = t_{0,2}/t_{0,3}$ given by Eq. (12) with β_k according to Eq. (9) is greater than found from the FE-analyses. Considering the alternative expressions for β_k according to Eq. (26) give, however, reasonably good agreement with results of the FE-analyses.

5. Discussion

For CLT at in-plane beam loading conditions, it has in Section 4 been shown that the internal force distribution found from FE-analyses is significantly influenced by the element lay-up in terms of the relative longitudinal layer thicknesses. The forces and torsional moments are equal for the two crossing areas in the beam width direction for CLT 3s, due to symmetry. However, the forces and torsional moments in general vary between the four crossing areas in the beam width direction for CLT 5s. For CLT 5s beams and the special case of an internal longitudinal layer having twice the thickness of the external longitudinal layers, i.e. $t_{0,2}/t_{0,1} = t_{0,2}/t_{0,3} = 2.0$, the forces and torsional moments are found to be equal for all crossing areas in the beam width direction. For

this specific lay-up is the ratio $t_{0,k}/n_{CA,k}$, between the longitudinal layer thickness $t_{0,k}$ and the number of crossing areas that the longitudinal layer shares with adjacent transversal laminations $n_{CA,k}$, constant for all k longitudinal layers.

Model A and Eqs. (1), (2), (4) and (5) are in [12] stated as being accurate for lay-ups having constant ratio $t_{0,k}/n_{CA,k}$ and as providing a sufficiently good approximation for CLT beams made of softwoods and with lay-ups that are used in practice. Commercially produced CLT elements typically have lay-ups with varying ratio $t_{0,k}/n_{CA,k}$ and ratios between internal and external longitudinal layer thicknesses in the range $0.5 \leqslant t_{0,2}/t_{0,1} = t_{0,2}/t_{0,3} \leqslant 1.0$. Within this range, the maximum values of the parallel to beam axis forces $F_{x,i,k}$ found from the FE-analyses were up to about 60% greater than for the reference case of constant ratio $t_{0,k}/n_{CA,k}$ and $t_{0,2}/t_{0,1} = t_{0,2}/t_{0,3} = 2.0$, see Fig. 7. For the torsional moments $M_{tor,i,k}$, maximum values found from the FE-analyses were up to about 30% greater than for the reference case of constant ratio $t_{0,k}/n_{CA,k}$.

The ratios between the maximum values of the torsional moments $M_{tor,i,k}$ for the centre-most crossing areas ($i = 2, 3$) found from the FE-analyses and according to model B with β_k according to Eq. (9) are 0.73–0.85, for element lay-ups with $0.5 \leqslant t_{0,2}/t_{0,1} = t_{0,2}/t_{0,3} \leqslant 1.0$. The corresponding ratios are instead 0.91–1.00 if considering weighting factors β_k according to Eq. (26). In other words, ignoring the approximate weighting factors β_k according to Eq. (26) and assuming $\beta_k = t_{0,k}/t_{net,0}$, as suggested in [15], gives for practically relevant element lay-ups an overestimation of the maximum torsional moment of about 20–35% compared to the results of the FE-analyses presented here. This (safe side) assumption and simplification may be reasonable to use for practical design purposes, since more user-friendly design equations may be obtained.

For CLT beams composed of longitudinal laminations of equal width b_0, the most stressed crossing areas are according to model A always the upper- and lower-most crossing area in the beam height direction since the forces $F_{x,i,k}$ increases with the distance from the neutral axis and since the torsional moments $M_{tor,i,k}$ are assumed to be equal for all crossing areas in the beam height direction. According to model B and the FE-results, however, the torsional moments $M_{tor,i,k}$ have their maximum value in the crossing areas located closest to the beam centreline. The location of the critical crossing area is hence not obvious and depends on the number of longitudinal laminations m in the beam height direction, the considered failure criterion and considered strength value/values with respect to the stress components τ_{xz} and τ_{tor}. This issue is further discussed in [15,16].

Within the work presented here, only CLT beams composed of either 3 or 5 layers were considered. Further studies of CLT beams composed of 7 layers should preferably also be conducted. It may also be relevant to study CLT beams with inverted layer orientation compared to the layer orientation considered within this work, i.e. element orientation such that the outermost layers are the transversal layers.

Another interesting aspect yet to be studied is the influence of varying lamination widths. In practice, CLT beams are often arbitrarily cut from large panels meaning that the width of (at least) the upper- and lower most laminations may differ compared to the nominal lamination width. Model B as presented here is in general valid also for the case of varying lamination widths, but with slight modifications to the equations given in Section 2.3 regarding the weighting factors α_i and forces and torsional moments acting in the crossing areas.

6. Conclusions

The analytical model as presented by Flaig & Blaß [12] has been used as a basis for design equations for CLT beams in the ongoing revision work of Eurocode 5. This model is, however, based on erroneous assumptions regarding the distributions of internal forces relevant for shear mode III failure, which has been pointed out in e.g. [8,14,15] and also shown here. Improvements of the original analytical model of Flaig & Blaß have been presented by Danielsson & Serrano [15].

The internal force distributions according to the original model (model A) and the improved model (model B) have here been compared to 3D FE-analyses of 3- and 5-layered CLT beams, with focus on the forces and torsional moments acting in the crossing areas. The comparison supports the proposed improvements in model B regarding the distributions in the beam width and beam height directions of the forces $F_{x,i,k}$ and the distributions of the shear forces $V_{i,k}$ and the torsional moments $M_{tor,i,k}$ in the beam height direction. Concerning the distribution in the beam width direction of $V_{i,k}$, and consequently also $M_{tor,i,k}$, some discrepancies between model B and the FE-analyses were found.

A distribution of the shear forces based on the relative thicknesses of the k layers of longitudinal laminations according to $V_{i,k} = \alpha_i \beta_k V$ with $\beta_k = t_{0,k}/t_{net,0}$ was assumed in [15]. Distributions of shear forces found from the FE-analyses presented here differ partly from this assumption and alternative expressions for the weighting factors β_k, based on curve-fitting of the shear forces found from the FE-results, were proposed. Using this modification, model B as presented in [15] yields good agreement also for torsional moments and their distribution in the beam width direction as compared to the FE-analyses.

Acknowledgements

This work was financially supported by the Swedish Research Council Formas through grant 2016-01090 for the project *Cross Laminated Timber Beams – Rational Structural Analysis* and by the Croatian Science Foundation through project No. IP-2016-06-381 *VETROLIGNUM – Prototype of multi-purpose composite cross laminated timber-load bearing glass panel.* The support from COST Action FP1402 is also gratefully acknowledged.

References

[1] Brandner R, Dietsch P, Dröscher J, Schulte-Wrede M, Kreuzinger H, Sieder M. Cross laminated timber (CLT) diaphragms under shear: test configuration, properties and design. Constr Build Mater 2017;147:312–27.
[2] Jöbstl RA, Bogensperger T, Schickhofer G. In-plane shear strength of cross laminated timber. In: Proc. CIB-W18, CIB-W18/41-12-3, St Andrews, Canada; 2008.
[3] Bejtka I. Cross (CLT) and diagonal (DLT) laminated timber as innovative material for beam elements. Karlsruhe, Germany: KIT; 2011.
[4] Andreolli M, Tomasi R, Polastri A. Experimental investigation on in-plane behaviour of cross-laminated timber elements. In: Proc. CIB-W18, CIB-W18/45-12-4, Växjö, Sweden; 2012.
[5] Blaß HJ, Flaig M. Stabförmige Bauteile aus Brettsperrholz. Karlsruhe, Germany: KIT; 2012.
[6] Flaig M. Biegeträger aus Brettsperrholz bei Beanspruch in Plattebene. PhD thesis. Karlsruhe, Germany: KIT; 2013.
[7] Danielsson, H., Jelec, M., Serrano, E., 2017. Strength and stiffness of cross laminated timber at in-plane beam loading. Report TVSM-7164, Sweden: Div of Structural Mechanics, Lund University. Available for download at http://www.byggmek.lth.se/publications.
[8] Danielsson H, Serrano E, Jelec M, Rajcic V. In-plane loaded CLT beams – tests and analysis of element lay-up. In: Proc. INTER, INTER/50-12-2, Kyoto, Japan; 2017.
[9] Flaig M. Design of CLT beams with rectangular holes or notches. In: Proc. INTER, INTER/47-12-4, Bath, United Kingdom; 2014.
[10] Flaig M. In Plattenebene beanspruchte Biegeträger aus Brettsperrholz – Teil 1: Effektive Festigkeits- und Steifigkeitskennwerte für die Schubbemessung. Bautechnik 2015;92:741–9.
[11] Flaig M. In Plattenebene beanspruchte Biegeträger aus Brettsperrholz – Teil 2: Brettsperrholzträger mit angeschnittenen Rändern, Durchbrüchen oder Ausklinkungen. Bautechnik 2015;92:750–8.
[12] Flaig M, Blaß HJ. Shear strength and shear stiffness of CLT-beams loaded in plane. In: Proc. CIB-W18, CIB-W18/46-12-3, Vancouver, Canada; 2013.
[13] Flaig M, Blaß HJ. Bending strength of cross laminated timber loaded in plane. In: Proc. WCTE 2014, Quebec City, Canada; 2014.
[14] Jelec M, Rajcic V, Danielsson H, Serrano E. Structural analysis of in-plane loaded CLT beam with holes: FE-analysis and parameter studies. In: Proc. INTER, INTER/49-12-2, Graz, Austria; 2016.
[15] Danielsson H, Serrano E. Cross laminated timber at in-plane beam loading – prediction of shear stresses in crossing areas. Eng Struct 2018;171:921–7.
[16] Jelec M, Danielsson H, Serrano E, Rajcic V. Cross laminated timber at in-plane beam loading – new analytical model predictions and relation to EC5. In: Proc. INTER, INTER/51-12-5, Tallinn, Estonia; 2018.
[17] Dassault Systemes Simulia Corp. ABAQUS, User Documentation, Version 2017.